

UC Irvine

UC Irvine Previously Published Works

Title

Neutron-diffraction study of the magnetic ordering in superconducting NdRh₄B₄

Permalink

<https://escholarship.org/uc/item/6026k3v1>

Journal

Physical Review B, 26(1)

ISSN

2469-9950

Authors

Majkrzak, CF
Cox, DE
Shirane, G
[et al.](#)

Publication Date

1982-07-01

DOI

10.1103/physrevb.26.245

Copyright Information

This work is made available under the terms of a Creative Commons Attribution License, available at <https://creativecommons.org/licenses/by/4.0/>

Peer reviewed

Neutron-diffraction study of the magnetic ordering in superconducting NdRh_4B_4

C. F. Majkrzak, D. E. Cox, and G. Shirane

Department of Physics, Brookhaven National Laboratory, Upton, New York 11973

H. A. Mook

Solid State Division, Oak Ridge National Laboratory, Oak Ridge, Tennessee 37830

H. C. Hamaker, H. B. MacKay, Z. Fisk, and M. B. Maple

Institute for Pure and Applied Physical Sciences, University of California, San Diego, La Jolla, California 92093

(Received 5 June 1981; revised manuscript received 18 December 1981)

The results of neutron-diffraction measurements are reported which confirm the development of long-range magnetic order in superconducting NdRh_4B_4 . Two distinct antiferromagnetic transitions occur below the superconducting phase-transition temperature $T_{\text{SC}}=5.4$ K, one at $T_{\text{MH}}\simeq 1.5$ K and the other at $T_{\text{ML}}\simeq 1.0$ K. In both phases, the body-centered tetragonal sublattice of Nd atoms orders antiferromagnetically with the Nd^{3+} moments aligned along the unique c axis. The magnetic moment is modulated sinusoidally along the [100] direction in the higher-temperature magnetic phase and along the [110] direction in the lower-temperature phase. The measured saturation moment is $3.4\pm 0.5\mu_B$. No ferromagnetic component could be detected in the higher-temperature magnetic phase within an experimental sensitivity of $0.3\mu_B$.

INTRODUCTION

The crystal structures of two classes of metallic rare-earth ternary compounds, the rare-earth (R) molybdenum chalcogenides RMO_6X_8 ($X=\text{S,Se}$) (Refs. 1 and 2) and the rare-earth rhodium borides RRh_4B_4 (Refs. 3 and 4), allow sufficient separation between the magnetic rare-earth ions that superconductivity and long-range magnetic order often occur simultaneously, as described in several recent review articles.⁵⁻⁹ Of the compounds in these two classes which have been studied thus far, those in which superconductivity and long-range magnetic order have been found to coexist microscopically order antiferromagnetically. For the two superconducting compounds ErRh_4B_4 (Refs. 10 and 11) and HoMo_6S_8 (Refs. 12 and 13), the development of long-range ferromagnetic order results in a re-entry to the normal state. Although neutron-diffraction determinations of the magnetic structures of several of the Chevrel-phase compounds have been reported, only ErRh_4B_4 of the rhodium borides has been studied in this way.

Measurements of the electrical resistance, heat capacity, upper critical magnetic field, and static magnetic susceptibility of NdRh_4B_4 by Hamaker *et al.*¹⁴ indicate that superconductivity and long-

range magnetic order coexist in this compound. We report here the results of neutron-diffraction measurements which confirm the occurrence of two distinct phases with long-range magnetic order below T_{SC} . In the higher-temperature magnetic phase, for which $T_{\text{MH}}\simeq 1.5$ K, the body-centered tetragonal (bct) sublattice of Nd moments orders antiferromagnetically with a sinusoidal modulation of the moment along the [100] direction. In the lower-temperature magnetic phase $T_{\text{ML}}\simeq 1.0$ K there is a change in the direction of the modulation wave vector to [110]. In both phases, the moments are aligned along the unique c axis.

EXPERIMENTAL DETAILS

The sample of NdRh_4B_4 was prepared by arc-melting NdB_6 and Rh in the relative proportion 1:6. The isotope ^{11}B was used since it has a substantially smaller absorption cross section for slow neutrons than does naturally occurring boron. In order to remove small traces of carbon which are found with the ^{11}B isotope, the NdB_6 was synthesized by precipitation from molten Al. The sample was made off-stoichiometry from the NdRh_4B_4 composition because the compound

$\text{RhB}_{1.1}$ which is also formed stabilizes the primitive tetragonal NdRh_4B_4 phase. In addition to the $\text{RhB}_{1.1}$, which has a hexagonal NiAs-type structure, a second impurity phase is present: NdRh_6B_4 , the structure of which is not as yet determined although its characteristic x-ray diffraction pattern is known. The resultant mixture has the chemical composition NdRh_6B_6 which requires the following weight fractions of the constituents: NdRh_6B_4 , 0.09; $\text{RhB}_{1.1}$, 0.25; NdRh_4B_4 , 0.66. This makeup is consistent with the relative intensities of x-ray powder-diffraction data. According to ac susceptibility measurements, the small amount of NdRh_6B_4 present in the sample orders magnetically at the relatively high temperature of about 4.9 K. The $\text{RhB}_{1.1}$, on the other hand, is neither superconducting nor magnetic between 0.06 and 20 K. This is discussed in more detail by Hamaker *et al.*¹⁴ The presence of these two impurities does not affect the determination of the magnetic structure of the NdRh_4B_4 phase whose magnetic diffraction peaks are quite distinct and display a unique temperature dependence as shown in the following section.

The sample, of volume 0.5 cm^3 ($\approx 4.7 \text{ g}$), used in the neutron-diffraction study was ground into a fine powder and loaded into a flat rectangular aluminum container mounted inside a liquid ^3He cryostat. In the present case, a flat sample geometry is preferable due to the relatively high

absorption of the compound. The transmission of the sample was measured to be 0.44 for a thickness of 0.1 cm. Diffraction measurements were performed at the Brookhaven High Flux Beam Reactor with a triple-axis spectrometer in the elastic scattering mode. Two configurations were used. One arrangement consisted of, in succession, a 20' in-pile beam collimator, pyrolytic graphite monochromator, 40' collimator, pyrolytic graphite filter (to suppress higher-order wavelengths), sample, 40' collimator, pyrolytic graphite analyzer, and 60' collimator preceding the detector. The incident neutron wave vector was 2.55 \AA^{-1} and the mosaic block distributions of monochromator and analyzer were of the order of 30' full width at half maximum. The other arrangement was similar to that described above but without the analyzer and at an incident wave vector of 2.635 \AA^{-1} .

RESULTS AND DISCUSSION

Complete diffraction patterns for scattering angles from 5° to 90° were obtained at temperatures above, below, and between the magnetic phase transitions. Structure factors obtained from the nuclear peak intensities of the primary phase measured by neutron diffraction above T_{MH} are consistent with those calculated on the basis of the tetragonal structure of NdRh_4B_4 reported by Vandenberg and Matthias,⁴ in which the magnetic Nd^{3+} ions occupy the corner and body-centered tetragonal positions with $a = 5.333 \text{ \AA}$ and $c = 7.468 \text{ \AA}$. Figure 1 shows diffraction data at three temperatures over the angular range where magnetic peaks were observed. The poor signal-to-noise ratio of the magnetic scattering in particular can be attributed to three principal factors: the relatively high-absorption cross section of the compound, the dilute concentration of magnetic moments (one Nd^{3+} atom for every nine atoms), and the relatively low average moment of Nd in this compound (as deduced below). The intensity of the larger impurity peak shown in Fig. 1 is approximately 14 times weaker than the strongest NdRh_4B_4 nuclear peak (103) which occurs at $2\theta = 66.24^\circ$ (and therefore does not appear in the figure).

Consider first the new peaks which are present at $T = 0.62 \text{ K}$. These cannot be indexed in terms of the chemical cell or any simple enlarged cell, thereby ruling out a simple ferromagnetic or antiferromagnetic arrangement. However, they can all be accounted for as satellites about the (100), (111), and (102) positions. The absence of a single satel-

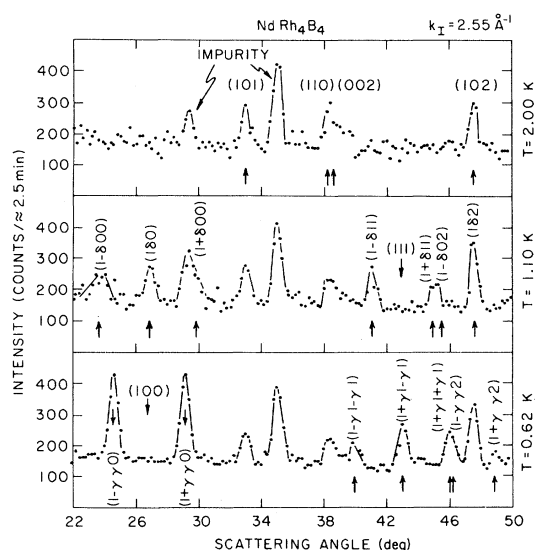


FIG. 1. Neutron-diffraction data above and below the magnetic phase-transition temperatures for the angular range over which magnetic peaks were observed. δ and γ label magnetic satellites and are defined in the text.

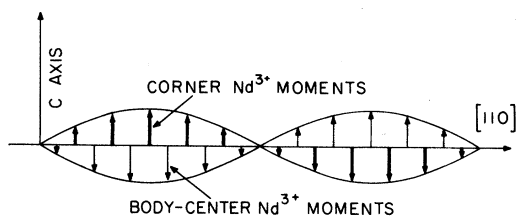


FIG. 2. Sinusoidal variation of the moments of the corner and body-centered Nd^{3+} ions along the $[110]$ direction in the lower-temperature magnetic phase of NdRh_4B_4 .

lite about the (001) position at $2\theta = 18.99^\circ$ is evidence that the Nd^{3+} moments are aligned along the unique c axis. The measured positions and intensities of the satellites are consistent with a body-centered tetragonal, antiferromagnetic sublattice of Nd^{3+} moments which are sinusoidally modulated along the $[110]$ direction, as pictured in Fig. 2, with a modulation wave vector of magnitude $|\vec{q}_{\text{ML}}| = 0.139 \text{ \AA}^{-1}$.

In the higher-temperature magnetic phase, the diffraction pattern at $T = 1.1 \text{ K}$ shows three satellites about (100) and (102) and two satellites about (111) , in contrast to the two satellites about (100) and (102) and the three satellites about (111) ob-

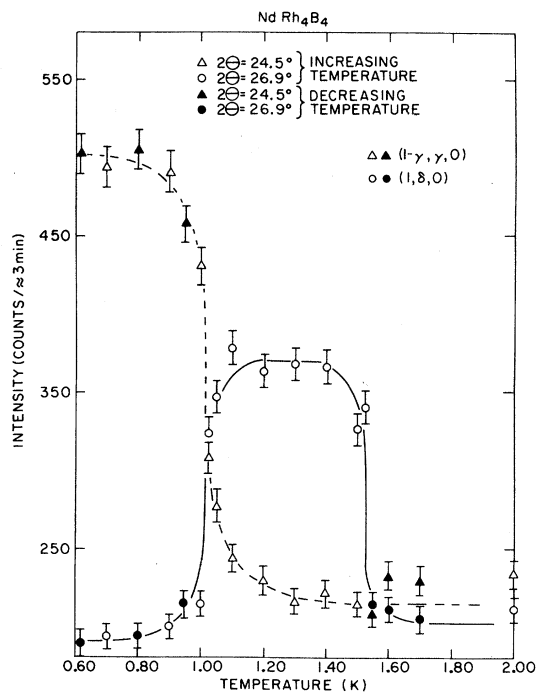


FIG. 3. Temperature dependence of the peak intensity of a representative satellite from each of the two magnetic phases. The background level is 189.0 ± 14.0 counts at 0.60 K .

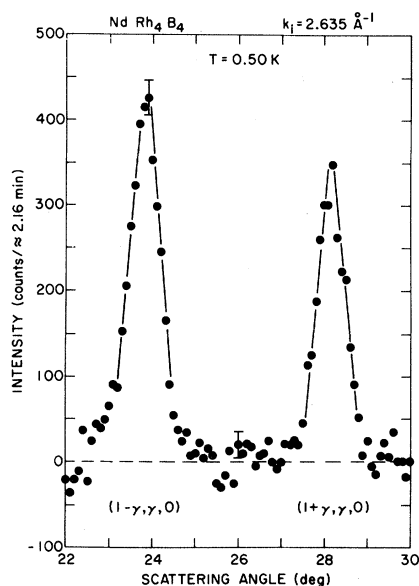


FIG. 4. Neutron-diffraction data showing the two satellites of (100) in the lower-temperature magnetic phase. Background and impurity contamination have been subtracted out.

served in the lower-temperature magnetic phase. As in the 0.62-K pattern, no satellite is observed about (001) . It can be inferred from these data that the magnetic structure is once again that of a sinusoidally modulated body-centered antiferromagnet with the Nd^{3+} moments alternately parallel and antiparallel to the c axis but with a modulation wave vector $|\vec{q}_{\text{MH}}| = 0.135 \text{ \AA}^{-1}$ directed along $[100]$ rather than $[110]$. In Fig. 1 (and also Fig. 3 and Table I) the quantities δ and γ are used to label satellites where $\delta \equiv |\vec{q}_{\text{MH}}|$ in units of $a^* = 2\pi/a$ ($\delta = 0.115$) and $\gamma \equiv |\vec{q}_{\text{ML}}|/\sqrt{2}$ in units of a^* ($\gamma = 0.083$).

Table I compares the observed peak positions and integrated intensities to those calculated on the basis of the model for the magnetic structures proposed above. For both the lower- and higher-temperature magnetic phases, agreement between the theoretical and measured angular positions is good and within the experimental uncertainty in scattering angles of $\approx 0.2^\circ$. In order to make a more reliable comparison of integrated intensities, additional data were obtained. Figure 4 shows some of these additional data corrected for background and underlying impurity peaks. The theoretical and measured integrated intensities in each of the two magnetic phases are, within the quoted experimental uncertainty, consistent.

It should be noted that within experimental error $|\vec{q}_{\text{ML}}|$ is $\frac{1}{12}$ the length of the (110) reciprocal-

TABLE I. Comparison of the observed to the theoretical peak positions and integrated intensities I corresponding to the model for the magnetic structures of NdRh_4B_4 proposed in the text. The angular dependence of the Nd^{3+} form factor was obtained from Ref. 15. Angles are given in degrees and intensities in arbitrary units.

HKL	$2\theta_{\text{obs}}$	$2\theta_{\text{calc}}$	I_{obs}	I_{calc}
Higher-temperature magnetic phase of NdRh_4B_4 : $k_i = 2.55 \text{ \AA}^{-1}$, $\mu_{\text{max}} = 3.4\mu_B$				
(1- δ ,0,0)	23.60	23.60	41 ± 8	43
(1, δ ,0)	26.90	26.89	57 ± 8	66
(1+ δ ,0,0)	30.00	29.85	27 ± 8	27
(1- δ ,1,1)	41.00	40.96	37 ± 10	45
(1+ δ ,1,1)	45.00	45.08	33 ± 10	46
(1- δ ,0,2)	45.40	45.66	15 ± 5	15
(1, δ ,2)	47.50	47.60		
Lower-temperature magnetic phase of NdRh_4B_4 : $k_i = 2.55 \text{ \AA}^{-1}$, $\mu_{\text{max}} = 3.4\mu_B$				
(1- γ , γ ,0)	24.50	24.55	79 ± 3	79
(1+ γ , γ ,0)	29.00	29.08	58 ± 3	57
(1- γ ,1- γ ,1)	40.00	40.00	21 ± 5	24
(1+ γ ,1- γ ,1)	43.00	43.13	41 ± 10	42
(1+ γ ,1+ γ ,1)	46.00	45.98	40 ± 10	34
(1- γ , γ ,2)	46.00	46.21		

lattice vector. A commensurate wave vector might result from antiphase domains rather than a sinusoidal modulation, in which case higher-order diffraction harmonics should appear. In particular, the third harmonic should be about $\frac{1}{10}$ as strong as the fundamental satellite. No higher-order harmonics were observed.

In both the lower- and higher-temperature magnetic phases, the widths of the satellites (as determined from more accurate data) are those given by the resolution of the spectrometer, which shows that the magnetic correlations are long range, with a minimum correlation range of 300 \AA . The temperature dependence of the intensity of a representative satellite from each of the two magnetic phases is shown in Fig. 3. By comparing the intensities of the (1- γ , γ ,0) satellite and the (101) nuclear reflection in the lower-temperature magnetic phase at 0.62 K, we calculate that the maximum amplitude of the Nd^{3+} magnetic moment at saturation is 3.4 ± 0.5 Bohr magnetons, whereas the free-ion value is $3.27\mu_B$.

As mentioned in the Introduction, those superconducting compounds which eventually develop long-range ferromagnetic order do so at the expense of the superconducting state. More precisely, in ErRh_4B_4 and HoMo_6S_8 the competition between ferromagnetism and superconductivity produces a compromise long-wavelength oscillatory

magnetization at intermediate temperatures.^{11,13,16,17} As the magnetic state develops with decreasing temperature, the superconductivity is destroyed. At low temperatures, the compounds are pure ferromagnets. Very recently, Thomlinson *et al.*¹⁸ have found that in the case of DyMo_6S_8 , which orders antiferromagnetically in the superconducting state in zero-applied magnetic field, the application of a field less than the upper critical field for superconductivity results in the development of long-range ferromagnetic order coexistent

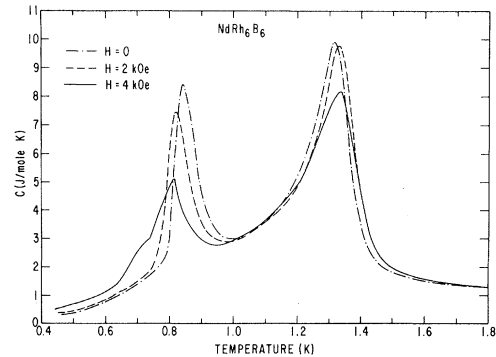


FIG. 5. Heat capacity C vs temperature of NdRh_6B_6 containing the primary phase NdRh_4B_4 and the impurity phases $\text{RhB}_{1,1}$ and NdRh_6B_4 in various applied magnetic fields.

with the superconducting state. Nevertheless, it cannot be concluded that the induced ferromagnetism is coexisting with the superconductivity in the same manner as the antiferromagnetism.¹⁹

It is of interest to note that the magnetization measurements of Hamaker *et al.*¹⁴ give evidence for the development of a ferromagnetic component of the Nd³⁺ magnetization in the higher-temperature magnetic phase. The onset of a ferromagnetic component to the Nd³⁺ magnetization at T_{MH} might account for the depression of the upper critical field at T_{MH} , while a decrease of the ferromagnetic component (possibly to zero) at T_{ML} could be responsible for the abrupt increase of the upper critical field at T_{ML} .

Figure 5, in which the heat capacity of the NdRh₆B₆ neutron sample versus temperature is plotted in various applied magnetic fields H , provides additional evidence of a ferromagnetic component in the higher-temperature magnetic phase. With increasing H , the peak associated with the transition at T_{ML} is shifted to lower temperatures, whereas applied magnetic fields cause the opposite effect at T_{MH} . Since enhancement (depression) of the magnetic-ordering temperature by H is generally characteristic of ferromagnetism (antiferromagnetism),²⁰ we have another indication of fer-

romagnetic behavior in the higher-temperature phase.

However, measurements of the intensities of nuclear Bragg diffraction peaks in zero-applied magnetic field above T_{MH} , between T_{MH} and T_{ML} , and below T_{ML} revealed no significant differences. Calculation shows that the uncertainties in the measured intensities place an upper limit of the order of $0.3\mu_B$ on the magnitude of a ferromagnetic component in the higher-temperature magnetic phase.

ACKNOWLEDGMENTS

We would like to thank W. Thomlinson for many helpful discussions. Research at Brookhaven was supported by the Division of Basic Energy Sciences, U. S. Department of Energy, under Contract No. DE-AC02-76CH00016. Research at Oak Ridge was supported by the U. S. Department of Energy under Contract No. W-7405-ENG-26. Research at the Institute for Pure and Applied Physical Sciences, La Jolla, was supported by the U. S. Department of Energy under Contract No. DE-AT0376-ER-70227 (HCM, HBM, and MBM) and by the National Science Foundation, Grant No. NSF/DMR 77-08469 (ZF).

¹Ø. Fischer, A. Treyvaud, R. Chevrel, and M. Sergent, *Solid State Commun.* **17**, 21 (1975).

²R. N. Shelton, R. W. McCallum, and H. Adrian, *Phys. Lett.* **56A**, 213 (1976).

³B. T. Matthias, E. Corenzwit, J. M. Vandenberg, and H. E. Barz, *Proc. Nat. Acad. Sci. U.S.A.* **74**, 1334 (1977).

⁴J. M. Vandenberg and B. T. Matthias, *Proc. Nat. Acad. Sci. U.S.A.* **74**, 1336 (1977).

⁵M. Ishikawa, Ø. Fischer, and J. Müller, *J. Phys. (Paris) Colloq.* **39**, C6-1379 (1978).

⁶M. B. Maple, in *Proceedings of the Indo-U.S. Seminar on the Science and Technology of the Rare Earth Materials*, edited by E. C. Subbarao and W. E. Wallace (Academic, New York, 1980), pp. 167–193.

⁷M. B. Maple, in *Proceedings of the International Conference on Ternary Superconductors, Lake Geneva, Wisconsin, 1980*, edited by G. K. Shenoy, B. D. Dunlap, and F. Y. Fradin (North-Holland, Amsterdam, 1981).

⁸D. E. Moncton, G. Shirane, and W. Thomlinson, *J. Magn. Magn. Mater.* **14**, 172 (1979).

⁹G. Shirane, W. Thomlinson, and D. E. Moncton, *Superconductivity in d- and f-Band Metals*, edited by H. Suhl and M. B. Maple (Academic, New York 1980), pp. 381–389.

¹⁰W. A. Fertig, D. C. Johnston, L. E. DeLong, R. W.

McCallum, M. B. Maple, and B. T. Matthias, *Phys. Rev. Lett.* **38**, 987 (1977).

¹¹D. E. Moncton, D. B. McWhan, J. Eckert, G. Shirane, and W. Thomlinson, *Phys. Rev. Lett.* **39**, 1164 (1977).

¹²M. Ishikawa and Ø. Fischer, *Solid State Commun.* **23**, 37 (1977).

¹³J. W. Lynn, D. E. Moncton, W. Thomlinson, G. Shirane, and R. N. Shelton, *Solid State Commun.* **26**, 493 (1978).

¹⁴H. C. Hamaker, L. D. Woolf, H. B. MacKay, Z. Fisk, and M. B. Maple, *Solid State Commun.* **31**, 139 (1979).

¹⁵W. C. Koehler and E. O. Wollan, *Phys. Rev.* **92**, 1380 (1953).

¹⁶D. E. Moncton, D. B. McWhan, P. H. Schmidt, G. Shirane, W. Thomlinson, M. B. Maple, H. B. MacKay, L. D. Woolf, Z. Fisk, and D. C. Johnston, *Phys. Rev. Lett.* **45**, 2060 (1980).

¹⁷J. W. Lynn, G. Shirane, W. Thomlinson, and R. N. Shelton, *Phys. Rev. Lett.* **46**, 368 (1981).

¹⁸W. Thomlinson, G. Shirane, D. E. Moncton, M. Ishikawa, and Ø. Fischer, *Phys. Rev. B* (in press).

¹⁹T. Krzyston, *J. Magn. Magn. Mater.* **15**, 1572 (1980).

²⁰K. P. Belov, *Magnetic Transitions* (Consultants Bureau, New York, 1961), pp. 41 and 131.